Journal of Aircraft
Vol. 47, No. 4, July–August 2010

Engineering Notes

Bodies Having Minimum Pressure Drag in Supersonic Flow: Investigating Nonlinear Effects

Karthik Palaniappan* and Antony Jameson†
Stanford University, Stanford, California 94305.

DOI: 10.2514/1.C031000

I. Introduction

THE life cycle of engineering design involves innovating to introduce a product, and when that is done, looking for ways to make it work better. Supersonic aerodynamics can be looked at with a similar perspective. Man has always wanted to fly faster. While the basic mechanics of supersonic flight was laid out in the 1950s, people are yet to find ways in which to make Supersonic flight more efficient.

One of the classic research problems in supersonic flight has been that of finding two-dimensional and axisymmetric profiles that have minimum pressure drag in supersonic flow. The two-dimensional sections are used as wing-profile sections, and the axisymmetric profiles are useful in that the distribution of the cross-sectional area is made to follow the optimum distribution (the area rule). This problem becomes redundant without suitable constraints. The minimum drag shape is a flat plate in two-dimensional flow and a needle-like profile in axisymmetric flow. This, however, is not a meaningful result. To make the problem more meaningful, the enclosed area/volume should be kept constant. The ends should also be kept pointed. This is to anchor the shocks firmly to the leading and trailing edges.

This problem has been solved in the fifties using a linear flow model. However, recent advances in computational fluid dynamics and aerodynamic shape optimization have made it possible for this problem to be analyzed using a nonlinear flow model. The results of this exercise are discussed in this paper.

II. Results from Classical Theory

Analytical solutions for the problem being studied have been obtained, assuming a linearized flow model. For the $2-d$ case the optimum profile is parabolic

$$y(x) = 3Ax(1-x), \qquad \tau = \frac{3A}{2} \tag{1}$$

where A is the area enclosed and τ is the thickness-chord ratio. The drag coefficient is given by

$$C_d = \frac{12A^2}{\sqrt{M^2-1}} \tag{2}$$

For the axisymmetric case, the profile shapes that solve this problem are the well-known Sears–Haack profiles, discovered independently by Sears (1947) [1] and Haack (1947). The derivation of the Sears–Haack profiles is outlined in the book by Ashley and Landahl [2] and also in an article by Ferrari [3]. The Sears–Haack profile is given by

$$y(x) = \sqrt{\frac{16V}{3\pi^2}}[4x(1-x)]^{\frac{3}{4}}, \qquad \tau = \sqrt{\frac{64V}{3\pi^2}} \tag{3}$$

where V is the enclosed volume and τ is the fineness ratio. The drag coefficient is given by

$$C_D = 24V \tag{4}$$

As can be observed, these profile shapes have some interesting properties. Firstly, they are unique solutions to the optimization problem. Moreover, they are just a function of the enclosed area/volume and not the Mach number.

III. Nonlinear Optimization via Control Theory

In this work, the adjoint method developed by Jameson and his associates during the last 15 years [4–7] is used. The aerodynamic shape optimization problem involves minimizing (or maximizing) a given cost function, with parameters that define the shape of the body as the design variables, usually of the form

$$I = \int_{\mathcal{B}_\xi} \mathcal{M}(w, S)\, \mathrm{d}\mathcal{B}_\xi \tag{5}$$

where w is the vector of flow state variables and S_{ij} are the coefficients of the Jacobian matrix of the transformation from physical space to computational space. $\mathcal{M}(w, S)$ in this case is just C_p, the pressure coefficient. There is also the constraint that the state variables at the computational points have to satisfy the flow equations, irrespective of the shape of the boundary

$$\int_{\mathcal{B}} n_i \phi^T f_i(w)\, \mathrm{d}\mathcal{B} = \int_{\mathcal{D}} \frac{\partial \phi^T}{\partial x_i} f_i(w)\, \mathrm{d}\mathcal{D} \tag{6}$$

or, when transformed to computational space

$$\int_{\mathcal{B}_\xi} n_i \phi^T S_{ij} f_j(w)\, \mathrm{d}\mathcal{B}_\xi = \int_{\mathcal{D}_\xi} \frac{\partial \phi^T}{\partial \xi_i} S_{ij} f_j(w)\, \mathrm{d}\mathcal{D}_\xi \tag{7}$$

where ϕ is any arbitrary test function.

Because Eq. (7) is true for any test function ϕ, ϕ can be chosen to be the adjoint variable ψ. Adding Eq. (7) to the cost function defined in Eq. (5) gives the following augmented cost function:

$$I = \int_{\mathcal{B}_\xi} \mathcal{M}(w, S)\, \mathrm{d}\mathcal{B}_\xi + \int_{\mathcal{B}_\xi} n_i \psi^T S_{ij} f_j(w)\, \mathrm{d}\mathcal{B}_\xi - \int_{\mathcal{D}_\xi} \frac{\partial \psi^T}{\partial \xi_i} S_{ij} f_j(w)\, \mathrm{d}\mathcal{D}_\xi \tag{8}$$

Taking a variation of the cost function described in Eq. (8)

$$\delta I = \int_{\mathcal{B}_\xi} \left(\frac{\partial \mathcal{M}}{\partial w} \delta w + \delta \mathcal{M}_{II} \right) \mathrm{d}\mathcal{B}_\xi + \int_{\mathcal{B}_\xi} n_i \psi^T \left(S_{ij} \frac{\partial f_j(w)}{\partial w} \delta w + \delta S_{ij} f_j(w) \right) \mathrm{d}\mathcal{B}_\xi - \int_{\mathcal{D}_\xi} \frac{\partial \psi^T}{\partial \xi_i} \left(S_{ij} \frac{\partial f_j(w)}{\partial w} \delta w + \delta S_{ij} f_j(w) \right) \mathrm{d}\mathcal{D}_\xi \tag{9}$$

Presented as Paper 2004-5383 at the 22nd Applied Aerodynamics Conference and Exhibit, Providence, RI, 16–19 August 2004; received 21 October 2009; 28 February 2010; 6 March 2010.

*Student, Department of Aeronautics and Astronautics, Currently Amoeba Technologies Inc., Austin, Texas. Senior Member AIAA.
†Professor, Department of Aeronautics and Astronautics. Fellow AIAA.

ψ is chosen such that the variation in the cost function δI does not depend on the variation of the solution δw; ψ is then a solution of the adjoint equations

$$\frac{\partial \mathcal{M}}{\partial w} = -n_i \psi^T S_{ij} \frac{\partial f_j(w)}{\partial w}, \quad \text{on } \mathcal{B}_\xi, \qquad \left(S_{ij} \frac{\partial f_j(w)}{\partial w}\right)^T \frac{\partial \psi}{\partial \xi_i} = 0, \quad \text{on } \mathcal{D}_\xi \tag{10}$$

One thus obtains an expression for the change in the cost function of the form

$$\delta I = \int_{\mathcal{B}_\xi} \mathcal{G} \delta \mathcal{F} d\mathcal{B}_\xi \tag{11}$$

where $\mathcal{F}(\xi)$ is a function defining the shape and $\mathcal{G}$ is the required gradient.

The gradient with respect to the design variables is obtained from the solutions to the adjoint equations by a reduced gradient formulation [6]. This is modified to account for the area/volume constraints. To preserve the smoothness of the profile, the gradient is smoothed by an implicit smoothing formula. This corresponds to redefining the gradient with respect to a weighted Sobolev inner product [5]. The optimum is then found by a sequential procedure in which the shape is modified in a descent direction defined by the smoothed gradient at each step, and the flow solution and the gradient are recalculated after each shape change.

IV. Results and Discussions

Convergence from Different Initial Conditions: The main test of the correctness of the optimization algorithm is to see if it converges to the same optimum profile regardless of what the initial profile is. Figures 1 and 2 show the optimization history from two different initial profile shapes for two-dimensional flow. They both enclose the same area. It can be seen that they converge to the same optimum profile. This helps to build confidence in the correctness of the optimization setup.

Optimum Profile Shapes: The results of the 2-D optimization can be seen in Fig. 3 and the results of the axisymmetric optimization can be seen in Fig. 4. As can be observed, the nonlinear optimum profiles are slightly different from the classical optimum profiles. They have a more rearward point of maximum thickness. The primary difference between a linearized flow model and a nonlinear model is the appearance of shocks at the leading edge in the case of the nonlinear flow model. Reducing the included angle at the leading edge and moving the point of maximum thickness backward is consistent with reducing the magnitude of the leading-edge shock. This results in a lower drag and at the same time brings the flow closer to the linear regime.

The difference is hardly noticeable for small thickness-chord/fineness ratios. This is simply an indicator of the fact that linear theory is a very good approximation for small fineness ratios. Moreover, the nonlinear optimum profiles for axisymmetric flow are a lot closer to their corresponding classical profiles than for 2-D flow. This is because of the three-dimensional relieving effect experienced in axisymmetric flow.

Variation with Mach Number: The optimum profile for 2-D flow changes with Mach number. The optimum shape for 2 M numbers is shown in Fig. 5. It is seen that the point of maximum thickness is farther rearward for the higher Mach number. This again is consistent with our earlier argument that the main goal of the nonlinear optimization is to reduce the magnitude of the leading-edge shock. Such a variation is not observed for axisymmetric optimum profiles. This is due to the fact that the drag coefficient is not sensitive to changes in Mach number in this case. This can also be seen from Eq. (4).

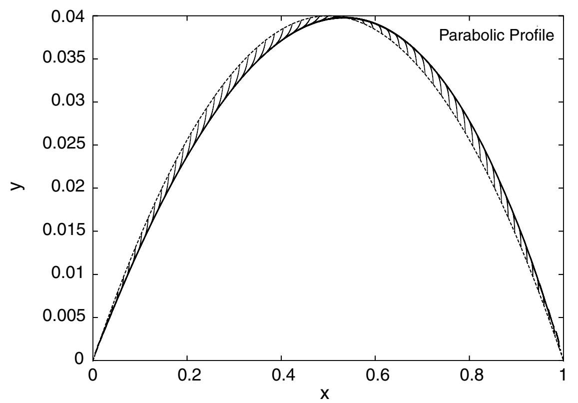

Fig. 1 Convergence of the optimization algorithm from a parabolic initial profile.

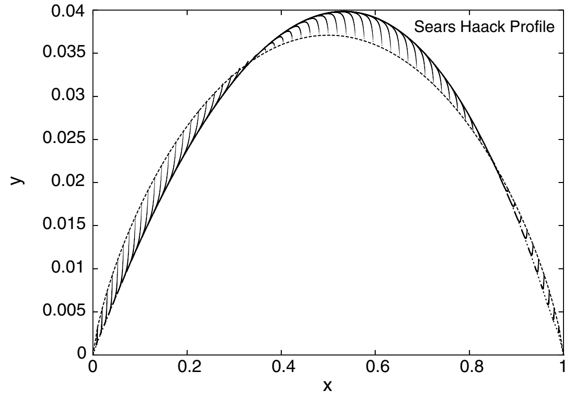

Fig. 2 Convergence of the optimization algorithm from a Sears–Haack initial profile.

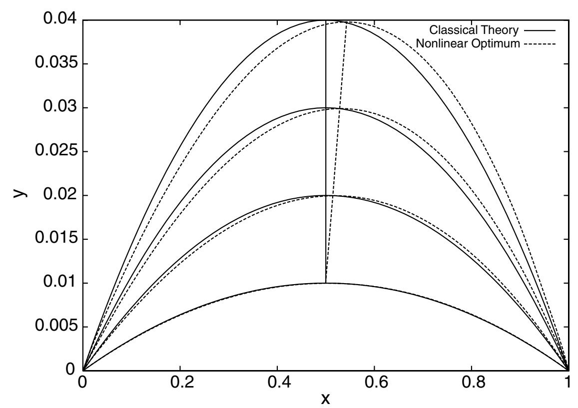

Fig. 3 Classical and nonlinear optimum profiles for 2-D flow.

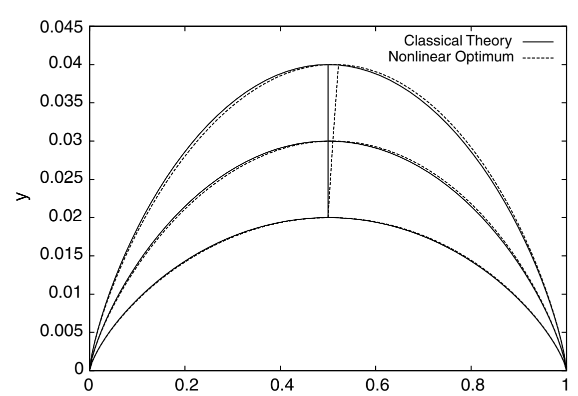

Fig. 4 Classical and nonlinear optimum profiles for axisymmetric flow.

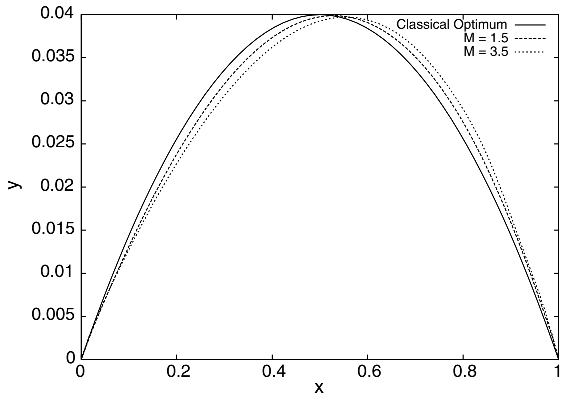

Fig. 5 Variation of 2-D optimum profiles with Mach number.

Discussion of Results: The main assumptions of linear theory are that the flow is isentropic, irrotational, and the perturbation velocities in the axial and normal directions are very small compared with the freestream velocity. These assumptions are valid everywhere except in the vicinity of the leading and the trailing edges, where there are stagnation points. Here, shocks cause entropy jumps. Moreover, the perturbation velocities are no longer small. Thus, the biggest change in the optimum profile shape is expected at these points. This is found to be true.

V. Conclusions

The minimum pressure drag problem was set up and solved using a nonlinear flow model. Optimization was carried out using the adjoint method. In both the two-dimensional case and the axisymmetric case, the resulting optimum profiles were compared with the optimum profiles obtained from linear theory. It was seen that they were different, though not vastly so. The optimum profiles are different for different Mach numbers in the case of two-dimensional flow. There is no Mach number dependence for axisymmetric flow. The optimal shapes become closer to their linear theory counterparts at low Mach numbers and small fineness ratios. Moreover, the differences are more obvious for two-dimensional sections than for axisymmetric profiles.

The main conclusion that is made is that the results from linear theory are very good as far as the optimum drag shapes are concerned. In this respect, it makes very good engineering sense to use results from linear theory for any preliminary design.

Acknowledgment

This work has been carried out under the support of the NASA Langley Research Center, under contract NAG-1-03046.

References

[1] Sears, W. R., “On Projectiles of Minimum Wave Drag,” *Quarterly of Applied Mathematics*, Vol. 4, No. 4, Jan. 1947.

[2] Ashley, H., and Landahl, M., *Aerodynamics of Wings and Bodies*, Dover, New York, 1985.

[3] Ferrari, C., “Bodies of Revolution having Minimum Pressure Drag,” *Theory of Optimum Aerodynamic Shapes*, edited by Angelo Miele Academic Press, New York, 1965, pp. 103–124.

[4] Jameson, A., “Aerodynamic Design via Control Theory,” *Journal of Scientific Computing*, Vol. 3, No. 3, 1988, pp. 233–260. doi:10.1007/BF01061285

[5] Jameson, A., “A Perspective on Computational Algorithms for Aerodynamic Analysis and Design,” *Progress in Aerospace Sciences*, Vol. 37, No. 2, 2001, pp. 197–243. doi:10.1016/S0376-0421(01)00004-5

[6] Jameson, A., and Kim, S., “Reduction of the Adjoint Gradient Formula in the Continuous Limit,” *41st AIAA Aerospace Sciences Meeting and Exhibit*, AIAA Paper 2003-0040, Reston, VA, Jan. 2003.

[7] Nadarajah, S., “The Discrete Adjoint Approach to Aerodynamic Shape Optimization,” Ph.D. Dissertation, Stanford Univ., Palo Alto, CA, 2003.